


JUNE 26 2015

Azimuth-elevation direction finding, using one four-component acoustic vector-sensor spread spatially along a straight line **FREE**

Yang Song; Kainam Thomas Wong 



Proc. Mtgs. Acoust. 23, 055001 (2015)

<https://doi.org/10.1121/2.0000053>



Articles You May Be Interested In

Azimuth-elevation direction finding using one four-component acoustic vector-sensor spread spatially as a parallelogram array

Proc. Mtgs. Acoust. (September 2016)

Near-field/far-field array manifold of an acoustic vector-sensor near a reflecting boundary

J. Acoust. Soc. Am. (June 2016)

Two biaxial velocity-sensors of non-identical orientation – their “spatial matched filter” beam-pattern’s pointing error

Proc. Mtgs. Acoust. (January 2019)



ASA

Advance your science and career as a member of the
Acoustical Society of America

[LEARN MORE](#)



169th Meeting of the Acoustical Society of America

Pittsburgh, Pennsylvania

18-22 May 2015

Signal Processing in Acoustics: Paper 4aSP4

Azimuth-elevation direction finding, using one four-component acoustic vector-sensor spread spatially along a straight line

Yang Song - *Universitat Paderborn*
Department of Electrical Engineering & Information Technology, Paderborn, North Rhin, Westphalia, Germany; yang.song@sst.upb.de

Kainam Thomas Wong - *Hong Kong Polytechnic University*
Department of Electronic & Information Engineering, Hong Kong; ktwong@ieee.org

An acoustic vector-sensor (a.k.a. a vector hydrophone for underwater applications) comprises one pressure-sensor plus three uniaxial velocity-sensors which are orthogonally oriented with regard to one other. Song & Wong [8] has analyzed how these four components can be placed arbitrarily in space to extend the three-dimensional array aperture, yet estimating a far-field incident acoustic emitter's azimuth-elevation direction-of-arrival. This work will focus on the particular array geometry whereby the four components are aligned on a straight line in three-dimensional space. This work will show how to estimate a far-field emitter's azimuth-elevation direction-of-arrival *unambiguously*, despite the four components' spatial separation, despite these separations' arbitrariness and sparseness.



1 Introduction - The Acoustic Vector-Sensor

A notable literature has emerged using a four-component acoustic vector-sensor to estimate the azimuth-elevation direction-of-arrival of acoustic emitters. Surveys this considerable literature are available from [4, 6, 7].

A four-component acoustic vector sensor constitutes of a pressure-sensor, plus three identical but perpendicular univariate *velocity*-sensors. These four components are often idealized as collocated. Mathematically, this acoustic *vector*-sensor (if placed at the origin of the three-dimensional Cartesian coordinates, without loss of generality) is characterized by this 4×1 array-manifold [1, 3, 5], in response to a unit-power incident acoustic wave that emits from the far field and that has traveled through an homogeneous isotropic medium:

$$\mathbf{a} := \begin{bmatrix} u(\theta, \phi) \\ v(\theta, \phi) \\ w(\theta) \\ 1 \end{bmatrix} := \begin{bmatrix} \sin(\theta) \cos(\phi) \\ \sin(\theta) \sin(\phi) \\ \cos(\theta) \\ 1 \end{bmatrix}, \quad (1)$$

where $\theta \in [0, \pi]$ denotes the elevation-angle measured from the vertical z -axis, $\phi \in [0, 2\pi)$ represents the azimuth-angle measured from the positive x -axis, $u(\theta, \phi)$ refers to the direction-cosine along the x -axis, $v(\theta, \phi)$ symbolizes the direction-cosine along the y -axis, and $w(\theta)$ signifies the direction-cosine along the z -axis. The first, second, and third components in $\mathbf{a}(\theta, \phi)$ correspond to the acoustic *velocity*-sensors aligned along the x -axis, the y -axis, and the z -axis, respectively. These three univariate velocity-sensors together measure the acoustic particle velocity vector, i.e., the gradient vector of the pressure field, thus specifying the negative of the incident wavefield's propagation direction. Lastly, the fourth component in $\mathbf{a}(\theta, \phi)$ corresponds to the pressure-sensor. These four components together satisfy the Frobenius-norm relationship of $\sqrt{\sum_{\ell=1,2,3} [\mathbf{a}]_{\ell}^2} = 1 = [\mathbf{a}]_4$, regardless of θ and ϕ . Here, $[\cdot]_{\ell}$ denotes the ℓ th element of the vector inside the square brackets.

One drawback of the above acoustic vector-sensor is its point-sized array aperture, on account of its four components' spatial collocation. However, if these four components are separated spatially, there would arise spatial phase factors among these components' measured data. Consequentially, the array-manifold of (1) would become invalid, and the pressure field's gradient vector would not be measured, and the incident wavefield's propagation direction could no longer be straight-forwardly obtainable by being read off from the gradient vector.

Nonetheless, [8] has shown how the four components may spread out arbitrarily in three-dimensional space (thus sampling the incident wavefield at *different* locations), while still achieve direction finding, and moreover to do so with enhanced accuracy.¹ This paper will focus on one particular array grid to spread out the four components – by placing them on a straight line in any permutation at any arbitrary inter-component spacings.

¹If the pressure sensor is absent, such that the acoustic vector-sensor degenerates to a triaxial velocity-sensor, please see [9].

2 Closed-Form Estimation Formulas for the Arrival Angles

2.1 Array Manifold of an Acoustic Vector-Sensor Spatially Distributed on a Straight Line, in Any Arbitrary Permutation, with Arbitrary Inter-Component Spacings

Align the four component-sensors at distinct locations along a straight line, in any permutation, with any inter-sensor spacing. Let this array axis be parallel to the x -axis, without loss of generality. Denote the pressure-sensor's location as (x_p, y_p, z_p) . The x -axis oriented velocity-sensor would then be located at $(x_p + \Delta_{px}, y_p, z_p)$; the y -axis oriented velocity-sensor would be placed at $(x_p + \Delta_{px} + \Delta_{xy}, y_p, z_p)$; and the z -axis oriented velocity-sensor would lie at $(x_p + \Delta_{px} + \Delta_{xy} + \Delta_{yz}, y_p, z_p)$. Here, Δ_{px} , Δ_{xy} , or Δ_{yz} may be of arbitrary value, positive or negative. This means that the four component-sensors may be aligned in any permutation. See Figure 2.1, wherein the velocity-sensor oriented along the x -axis, y -axis, and z -axis are respectively identified as V_x , V_y , and V_z , with the pressure-sensor as P .

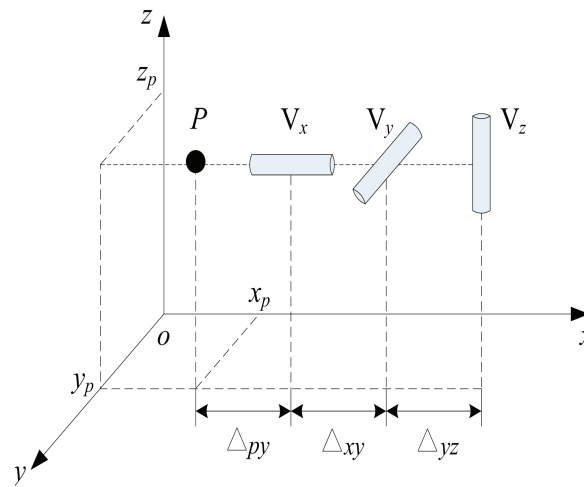


Figure 1: The four component-sensors aligned along the x -axis. Shown here is the special case where $\Delta_{px} > 0$, $\Delta_{xy} > 0$, and $\Delta_{yz} > 0$.

For this spatially spread configuration, the 4×1 array-manifold is no longer (1), but as follows:

$$\mathbf{a}_x = \begin{bmatrix} u e^{j \frac{2\pi}{\lambda} [(\Delta_{px} + x_p)u + y_p v + z_p w]} \\ v e^{j \frac{2\pi}{\lambda} [(\Delta_{xy} + \Delta_{px} + x_p)u + y_p v + z_p w]} \\ w e^{j \frac{2\pi}{\lambda} [(\Delta_{yz} + \Delta_{xy} + \Delta_{px} + x_p)u + y_p v + z_p w]} \\ e^{j \frac{2\pi}{\lambda} [x_p u + y_p v + z_p w]} \end{bmatrix}. \quad (2)$$

2.2 Eigen-Estimate of the Steering Vector

Subspace-based algorithms eigen-decompose the data-correlation matrix, to estimate the incident emitter's steering vector $\hat{\mathbf{a}}_x = c \mathbf{a}_x$, to within an *unknown* complex-value scalar c . That is, available from eigen-decomposing the data-correlation matrix would be

$$c \mathbf{a}_x = [p_x, p_y, p_z, p_p]^T, \quad (3)$$

where the superscript T denotes transposition.

2.3 Estimate of the Azimuth-Elevation Direction-of-Arrival

For the moment, consider asymptotic or noiseless conditions, which would lead to

$$\frac{p_x}{p_p} = u e^{j\frac{2\pi}{\lambda}(\Delta_{px}u)} \quad (4)$$

$$\frac{p_y}{p_p} = v e^{j\frac{2\pi}{\lambda}[(\Delta_{xy}+\Delta_{px})u]} \quad (5)$$

$$\frac{p_z}{p_p} = w e^{j\frac{2\pi}{\lambda}[(\Delta_{yz}+\Delta_{xy}+\Delta_{px})u]}. \quad (6)$$

From (4), two complementary estimators of u are obtainable:

- {i} For an extended aperture where $\frac{\Delta_{px}}{\lambda} > \frac{1}{2}$, a one-to-many relationship exists between $e^{j2\pi\frac{\Delta_{px}}{\lambda}u}$ and $u \in [-1, 1]$. Therefore,

$$\hat{u}_{\text{phs}} = \frac{1}{2\pi} \frac{\lambda}{\Delta_{px}} \angle \frac{p_x}{p_p} = m \frac{\lambda}{\Delta_{px}} + u \quad (7)$$

estimates u only ambiguously to within some (unknown) integer multiple ($m \times$) of the frequency-dependent $\pm \frac{\lambda}{\Delta_{px}}$, with m representing an integer to be evaluated.

- {ii} The frequency-independent

$$\hat{u}_{\text{mag}} = \left| \frac{p_x}{p_p} \right| = \pm u \quad (8)$$

estimates u only ambiguously as well, but to within a \pm sign.

The above two estimates (\hat{u}_{phs} and \hat{u}_{mag}) can disambiguate one other as follows:

- {a} For $\hat{u}_{\text{mag}} = u$, the cyclic ambiguity can be resolved via $\hat{m}_u^+ :=$

$$\arg \min_m \left\{ \left| \underbrace{\left(m \frac{\lambda}{\Delta_{px}} + \overbrace{\frac{1}{2\pi} \frac{\lambda}{\Delta_{px}} \angle \frac{p_x}{p_p}}^{=\hat{u}_{\text{phs}}} \right)}_{:=\epsilon_u^+(m)} - \overbrace{\left| \frac{p_x}{p_p} \right|}^{=\hat{u}_{\text{mag}}} \right| \right\}.$$

- {b} For $\hat{u}_{\text{mag}} = -u$, the cyclic ambiguity can be resolved via $\hat{m}_u^- :=$

$$\arg \min_m \left\{ \left| \underbrace{\left(m \frac{\lambda}{\Delta_{px}} + \overbrace{\frac{1}{2\pi} \frac{\lambda}{\Delta_{px}} \angle \frac{-p_x}{p_p}}^{=\hat{u}_{\text{phs}}} \right)}_{:=\epsilon_u^-(m)} - - \overbrace{\left| \frac{p_x}{p_p} \right|}^{=\hat{u}_{\text{mag}}} \right| \right\}.$$

- {c} To choose between $\hat{u}_{\text{mag}} = u$ versus $\hat{u}_{\text{mag}} = -u$: Choose $\hat{u}_{\text{mag}} = u$, if $\epsilon_u^+(\hat{m}_u^+) < \epsilon_u^-(\hat{m}_u^-)$. Choose $\hat{u}_{\text{mag}} = -u$, if $\epsilon_u^+(\hat{m}_u^+) \geq \epsilon_u^-(\hat{m}_u^-)$.

{d} u may now be *unambiguously* estimated as $\hat{u} =$

$$\begin{cases} \left(\hat{m}_u^+ + \frac{1}{2\pi} \angle \frac{p_x}{p_p} \right) \frac{\lambda}{\Delta_{px}}, & \text{if } \epsilon_u^+(\hat{m}_u^+) < \epsilon_u^-(\hat{m}_u^-). \\ \left(\hat{m}_u^- - \frac{1}{2\pi} \angle \frac{p_x}{p_p} \right) \frac{\lambda}{\Delta_{px}}, & \text{if } \epsilon_u^+(\hat{m}_u^+) \geq \epsilon_u^-(\hat{m}_u^-). \end{cases}$$

The estimates, \hat{v} and \hat{w} , may likewise be obtained as

$$\begin{aligned} \hat{v} &= \frac{p_y}{p_p} e^{-j \frac{2\pi}{\lambda} (\Delta_{xy} + \Delta_{px})} \hat{u} \\ \hat{w} &= \frac{p_z}{p_p} e^{-j \frac{2\pi}{\lambda} (\Delta_{yz} + \Delta_{xy} + \Delta_{px})} \hat{u} \end{aligned}$$

Finally, \hat{u} , \hat{v} , \hat{w} together produce the direction-of-arrival estimates:

$$\hat{\theta} = \arccos \hat{w}, \quad (9)$$

$$\hat{\phi} = \begin{cases} -\arccos \left(\frac{\hat{v}}{\sin(\hat{\theta})} \right), & \text{if } \frac{\hat{v}}{\sin(\hat{\theta})} < 0 \\ \arccos \left(\frac{\hat{v}}{\sin(\hat{\theta})} \right), & \text{if } \frac{\hat{v}}{\sin(\hat{\theta})} \geq 0. \end{cases} \quad (10)$$

These arrival-angle estimates are valid over a support-region spanning the entire spherical space of $\theta \in [0, \pi)$ and $\phi \in (-\pi, \pi]$. Therefore, direction finding has been achieved *unambiguously*, despite the four components' spatial separation, despite these separations' arbitrariness and sparseness.

3 Cramér-Rao Bound versus Inter-Component Spacing

The Enhanced accuracy of direction finding, obtained by spatially spreading the four-component acoustic vector-sensor, is investigated via Cramér-Rao bound analysis here.

To avoid distraction from these *non*-collocated components' array manifold, a simple statistical model will be used below for the signal and the noise: The emitted signal $s(t) = e^{j(\omega t + \epsilon)}$ is a pure tone at an angular frequency of ω , with an initial phase of ϵ . Both ω and ϵ are deterministic known constants.

At the m th time-instant of $t = mT_s$, a 4×1 data-vector $\tilde{\mathbf{z}}(mT_s)$ is collected by the four components:

$$\tilde{\mathbf{z}}(mT_s) = \tilde{\mathbf{a}}_x s(mT_s) + \tilde{\mathbf{n}}(mT_s), \quad (11)$$

where T_s refers to the time-sampling period, and $\tilde{\mathbf{n}}(t)$ denotes a 4×1 vector of additive zero-mean spatio-temporally uncorrelated Gaussian noise, with a known deterministic covariance-matrix of $\mathbf{\Gamma}_0 = \text{diag}(\sigma^2, \sigma^2, \sigma^2, \sigma^2)$. That is, σ^2 represents the known noise-variance at each component-sensor.

With M number of time-samples, the $4 \times M$ collected data-set equals

$$\begin{aligned} \mathbf{z} &= [\tilde{\mathbf{z}}(T_s)^T, \dots, \tilde{\mathbf{z}}(MT_s)^T]^T \\ &= \underbrace{\mathbf{s} \otimes \mathbf{a}}_{\text{def } \boldsymbol{\mu}} + \underbrace{[\tilde{\mathbf{n}}(T_s)^T, \dots, \tilde{\mathbf{n}}(MT_s)^T]^T}_{\text{def } \mathbf{n}} \end{aligned} \quad (12)$$

where $\mathbf{s} = e^{j\epsilon} [e^{jT_s\omega}, e^{j2T_s\omega}, \dots, e^{jMT_s\omega}]^T$, \otimes symbolizes the Kronecker product, $\boldsymbol{\mu}$ represents a $4M \times 1$ noise vector with a spatio-temporal covariance matrix of $\mathbf{\Gamma} = \mathbf{I}_M \otimes \mathbf{\Gamma}_0$, and \mathbf{I}_M denotes an $M \times M$ identity matrix. Therefore, $\mathbf{z} \sim \mathcal{N}(\boldsymbol{\mu}, \mathbf{\Gamma})$.

Collect all deterministic unknown entities into a 2×1 vector, $\boldsymbol{\psi} = [\theta, \phi]^T$. The resulting 2×2 Fisher

information matrix, \mathbf{J} , would have a (i, j) th entry equal to (equation (8.34) in [2])

$$[\mathbf{J}]_{i,j} = 2\text{Re} \left[\left(\frac{\partial \boldsymbol{\mu}}{\partial [\boldsymbol{\psi}]_i} \right)^H \boldsymbol{\Gamma}^{-1} \left(\frac{\partial \boldsymbol{\mu}}{\partial [\boldsymbol{\psi}]_j} \right) \right] + \text{Tr} \left[\boldsymbol{\Gamma}^{-1} \frac{\partial \boldsymbol{\Gamma}}{\partial [\boldsymbol{\psi}]_i} \boldsymbol{\Gamma}^{-1} \frac{\partial \boldsymbol{\Gamma}}{\partial [\boldsymbol{\psi}]_j} \right] \quad (13)$$

where $\text{Re}[\cdot]$ denotes the real-value part of the entity inside $[\cdot]$, and $\text{Tr}[\cdot]$ represents the trace operator. To focus on the influence of the inter-component spacings' effect on the Cramér-Rao bounds, take $\Delta_{px} = \Delta_{xy} = \Delta_{yz} = \Delta$. Without loss of generality set $(x_p, y_p, z_p) = (0, 0, 0)$.

The above equations, after some mundane mathematical manipulations, give $[\mathbf{J}]_{1,1}$, $[\mathbf{J}]_{1,2}$, $[\mathbf{J}]_{2,1}$, $[\mathbf{J}]_{2,2}$ on the next page. From these expressions, the Cramér-Rao bounds are obtained and presented in (14)-(15). These Cramér-Rao bounds would degenerate to those of a collocated acoustic vector-sensor as presented in Table IV of [4].

$$[\mathbf{J}]_{1,1} = \frac{2M}{\sigma^2} \left\{ \pi^2 \left(\frac{\Delta}{\lambda} \right)^2 \sin^2(2\phi) \sin^2(2\theta) + 4\pi^2 \left(\frac{\Delta}{\lambda} \right)^2 \cos^2(\theta) \cos^2(\phi) [\cos^2(\phi) \sin^2(\theta) + 9 \cos^2(\theta)] + 1 \right\}$$

$$[\mathbf{J}]_{2,2} = \frac{2M}{\sigma^2} \sin^2(\theta) \left\{ \pi^2 \left(\frac{\Delta}{\lambda} \right)^2 [16 \sin^4(\phi) + \sin^2(2\phi)] \sin^2(\theta) + 36\pi^2 \left(\frac{\Delta}{\lambda} \right)^2 \sin^2(\phi) \cos^2(\theta) + 1 \right\}$$

$$[\mathbf{J}]_{1,2} = [\mathbf{J}]_{2,1} = \frac{M}{2} \left(\frac{\pi \Delta}{\sigma \lambda} \right)^2 \sin(\phi) \sin(2\theta) \{6 \cos(3\phi) \sin^2(\theta) - \cos(\phi) [29 \cos(2\theta) + 43]\}$$

$$\begin{aligned} \text{CRB}(\theta) &= [\mathbf{J}^{-1}]_{(1,1)} \\ &= \frac{8\sigma^2}{M} \frac{\pi^2 \left(\frac{\Delta}{\lambda} \right)^2 [(16 \sin^4(\phi) + \sin^2(2\phi)) \sin^2(\theta) + 36 \sin^2(\phi) \cos^2(\theta)] + 1}{\pi^2 \left(\frac{\Delta}{\lambda} \right)^2 [24 \cos(4\phi) \sin^4(\theta) - 128 \cos(2\phi) \sin^2(\theta) (\cos(2\theta) + 2) + 236 \cos(2\theta) + 29 \cos(4\theta) + 311] + 16} \end{aligned} \quad (14)$$

$$\begin{aligned} \text{CRB}(\phi) &= [\mathbf{J}^{-1}]_{(2,2)} \\ &= \frac{\sigma^2}{2M} \frac{\pi^2 \left(\frac{\Delta}{\lambda} \right)^2 \csc^4(\theta) \cos^2(\phi) [(13 \cos(2\theta) + 23) \cot^2(\theta) - 6 \cos(2\phi) \cos^2(\theta)] + \csc^6(\theta)}{2\pi^2 \left(\frac{\Delta}{\lambda} \right)^2 [\cos^2(\phi) (3 \cos(2\phi) + 13) - 2(6 \cos(2\phi) + 11) \csc^2(\theta) + 18 \csc^4(\theta)] + \csc^4(\theta)} \end{aligned} \quad (15)$$

The above derived formulas (14)-(15) are plotted in Figure 2, at $\text{SNR} = 0\text{dB}$, $\omega = 1000\pi$, $\theta = \frac{\pi}{6}$, and $\phi = \frac{\pi}{4}$. Figure 2 confirms that the Cramér-Rao bounds steadily decrease, as Δ increases.

Similar trends can be readily derived for the case where all component-sensors are aligned instead along the y -axis or the z -axis.

4 Conclusion

This paper has shown how an acoustic vector-sensor's four components may be spatially distributed arbitrarily on a straight line, in order to extend the spatial aperture to improve the direction finding accuracy. This straight-line case represents one special case of the more general result in [8].

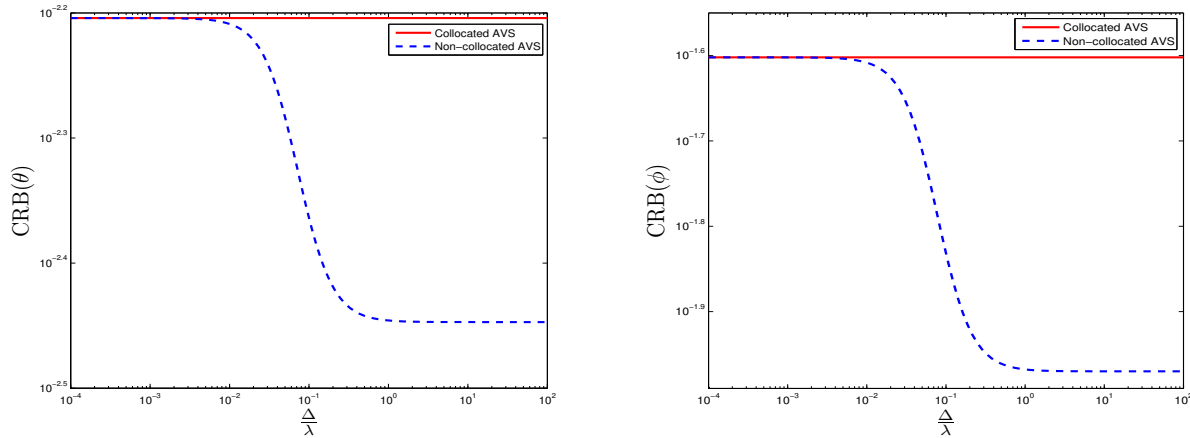


Figure 2: $\text{CRB}(\theta)$ and $\text{CRB}(\phi)$ versus $\frac{\Delta}{\lambda}$, at $\text{SNR} = 0\text{dB}$, $M = 80$, $\theta = \frac{\pi}{6}$, and $\phi = \frac{\pi}{4}$.

References

- [1] A. Nehorai & E. Paldi, "Acoustic vector-sensor array processing," *IEEE Transactions on Signal Processing*, vol. 42, no. 10, pp. 2481-2491, September 1994.
- [2] H. L. Van Trees, *Detection, Estimation, and Modulation Theory, Part IV: Optimum Array Processing*, New York, U.S.A.: Wiley, 2002.
- [3] J. A. McConnell, "Analysis of a compliantly suspended acoustic velocity sensor," *Journal of the Acoustical Society of America*, vol. 113, no. 3, pp. 1395-1405, March 2003.
- [4] P. K. Tam & K. T. Wong, "Cramér-Rao bounds for direction finding by an acoustic vector-sensor under non-ideal gain-phase Responses, Non-Collocation, or Non-Orthogonal Orientation," *IEEE Sensors Journal*, vol. 9, no. 8, pp. 969-982, August 2009.
- [5] Y. I. Wu, K. T. Wong & S.-K. Lau, "The acoustic vector-sensor's near-field array-manifold," *IEEE Transactions on Signal Processing*, vol. 58, no. 7, pp. 3946-3951, July 2010.
- [6] K. T. Wong, "Acoustic vector-sensor "blind" beamforming & geolocation for FFH-sources," *IEEE Transactions on Aerospace and Electronic Systems*, vol. 46, no. 1, pp. 444-449, January 2010.
- [7] Y. I. WU & K. T. Wong, "Acoustic near-field source localization by two passive anchor nodes," *IEEE Transactions on Aerospace and Electronic Systems*, vol. 48, no. 1, pp. 159-169, January 2012.
- [8] Y. Song & K. T. Wong, "Azimuth-elevation direction finding using a microphone and three orthogonal velocity sensors as a non-collocated subarray," *Journal of the Acoustical Society of America*, vol. 133, no. 4, pp. 1987-1995, April 2013.
- [9] Y. Song & K. T. Wong, "Acoustic direction finding using a spread triaxial velocity sensor," *IEEE Transactions on Aerospace and Electronic Systems*, vol. 51, no. 2, April 2015.